Journal of Inflammation Research

Dovepress
Taylor & Francis Group

Open Access Full Text Article

ORIGINAL RESEARCH

HMGB1 Inhibition Alleviates Chronic Nonbacterial Prostatitis by Suppressing M1 Polarization of Macrophages

Jilong Zhou[1,*], Lihui Ding[1,2,*], Juan Chen[2], Chen Chen[1], Ping Jiang[2], Zongwei Mei[1], Qing Jiang[1], Xiaoliang Hua[1,3]

[1]Department of Urology, The Second Affiliated Hospital of Chongqing Medical University, Chongqing, People's Republic of China; [2]The Ministry of Education Key Laboratory of Laboratory Medical Diagnostics, The College of Laboratory Medicine, Chongqing Medical University, Chongqing, 400016, People's Republic of China; [3]Hubei Key Laboratory of Urological Diseases, Zhongnan Hospital of Wuhan University, Wuhan, 430071, People's Republic of China

*These authors contributed equally to this work

Correspondence: Qing Jiang; Xiaoliang Hua, Department of Urology, The Second Affiliated Hospital of Chongqing Medical University, No. 74 Linjiang Road, Yuzhong District, Chongqing, 400010, People's Republic of China, Tel/Fax +86 023 6369 3222, Email 300899@hospital.cqmu.edu.cn; hua_xiaoliang@cqmu.edu.cn

Background and Objective: Chronic Prostatitis/Chronic Pelvic Pain Syndrome (CP/CPPS) poses a significant threat to male urinary health and has an unclear pathogenesis. High-mobility group box 1 (HMGB1), a danger-associated molecular pattern that has been identified as a key mediator in various inflammatory diseases. However, its role in CP/CPPS remains unclear. This study aimed to investigate HMGB1's potential contributions to the pathogenesis of CP/CPPS, offering new perspectives for innovative treatments.

Materials and Methods: We have successfully extracted prostate antigens from Sprague–Dawley rat prostate tissue and established an experimental autoimmune prostatitis (EAP) mouse model in non-obese diabetic (NOD) mice. Subsequently, EAP mice were treated with recombinant HMGB1 protein (rmHMGB1) or the HMGB1-specific inhibitor glycyrrhizin for 14 days. Behavioral test was performed to assess the chronic pelvic pain. Hematoxylin and eosin (H&E) staining was employed to assess the extent of inflammatory cell infiltration in the prostate, and enzyme-linked immunosorbent assay (ELISA) was performed to assess levels of inflammatory cytokines. Co-immunofluorescence was used to analyze the functional phenotype of macrophages and spatial localization of HMGB1 in prostate of EAP mice. To further validate these findings, we conducted in vitro experiments. In these experiments, lipopolysaccharide (LPS) was used to induce an inflammatory environment in RAW264.7 cells. Interventions included administering rmHMGB1, silencing HMGB1 gene expression with siRNA, and treating cells with the TRAF6 inhibitor C25-140. After interventions, Western blot and immunofluorescence were employed to evaluate the impact on M1 macrophage polarization and inflammation.

Results: In this study, we demonstrate that HMGB1 is highly expressed in the prostate tissues of EAP mice. Treating EAP mice with rmHMGB1 significantly increased prostate histological scores (2.83 vs 1.83, $p < 0.05$) and the sensitivity to pain stimuli, as evidenced by a higher response frequency to von Frey filament stimulation at 4 g (68.33% vs 53.33%, $p < 0.05$). This treatment also increased the levels of inflammatory proteins IL-6 and TNF-α. In contrast, suppressing HMGB1 with glycyrrhizin significantly reduced inflammation, as indicated by decreased histological scores (0.50 vs 2.17, $p < 0.05$), and attenuated pain sensitivity, as evidenced by a lower response frequency to von Frey filament stimulation at 4 g (30.83% vs 52.50%, $p < 0.05$). Glycyrrhizin treatment also reduced IL-6 and TNF-α levels. Furthermore, the proportion of $CD11b^{+}iNOS^{+}$ cells, indicative of M1 macrophage polarization, was significantly reduced after glycyrrhizin treatment. In vitro, HMGB1 can regulate the activity of TRAF6 by partially modulating its ubiquitination and degradation, thereby amplifying TRAF6-mediated NF-κB activation, promoting M1 macrophage polarization, and exacerbating inflammation.

Discussion and Conclusions: HMGB1 can enhance TRAF6-mediated NF-κB activation, thereby driving M1 macrophage polarization and exacerbating prostate inflammation in EAP mice. Inhibiting HMGB1 expression with glycyrrhizin can suppress M1 polarization of macrophages to alleviate prostate inflammation. This study suggests that targeting the HMGB1/TRAF6/NF-κB signaling pathway may be an effective therapeutic approach for CP/CPPS.

Keywords: HMGB1, chronic nonbacterial prostatitis, macrophages, TRAF6, inflammation

Received: 27 November 2024
Accepted: 26 April 2025
Published: 25 May 2025

Introduction

Prostatitis is among the most frequently encountered conditions in urological practice. According to epidemiological data, the prevalence of prostatitis-like symptoms ranges from 2.2% to 9.7%, with an average incidence rate of 8.2%.[1] According to the classification established by the National Institutes of Health (NIH), prostatitis is divided into four categories. Among these, Type III CP/CPPS is the primary form of prostatitis, comprising over 90% of all cases.[2] It presents with a diverse symptomology, including persistent pelvic discomfort, urinary difficulties, sexual dysfunction, fatigue, and memory impairment, significantly impacting the health and quality of life of affected individuals.[3–5] Due to the complex pathogenesis of CP/CPPS, effective treatment strategies remain limited. Numerous studies have suggested that the pathogenesis of CP/CPPS may be associated with multiple factors, including autoimmune imbalances, neurogenic factors, psychosocial stress, direct infection.[6–8]

CP/CPPS often lacks an identifiable bacterial etiology. Recent advancements in the field have highlighted the pivotal role of autoimmune mechanisms in the pathogenesis and progression of CP/CPPS, positioning them as a focal point of contemporary research endeavors. Traditionally viewed through the lens of its secretory functions, the prostate gland also possesses a remarkably robust immune apparatus. It contains a diverse array of immune cells, including macrophages, T and B lymphocytes, and mast cells, predominantly localized within the gland's stromal compartments.[9,10] This immune surveillance system suggests a protective role against pathogens. However, its dysregulation may significantly contribute to the chronic inflammation seen in CP/CPPS. Pathological examinations of prostate tissues from CP/CPPS patients have consistently shown significant infiltration of neutrophils, monocytes, and T lymphocytes.[11,12] These findings are supported by studies documenting an increased presence of these cells, along with macrophages and B lymphocytes, in prostatic fluid and semen samples of affected individuals.[13,14] These observations highlight the critical role of these immune cells in initiating and sustaining the inflammatory response characteristic of CP/CPPS.

HMGB1 is a highly conserved nuclear DNA-binding protein with diverse biological functions, including the promotion of nuclear DNA damage repair, immune regulation, and enhancement of autophagy.[15] Previous studies have identified elevated HMGB1 expression in prostate epithelial cells and inflammatory cells in patients with benign prostatic hyperplasia combined with prostatitis.[16] Nevertheless, the precise role and function of HMGB1 in CP/CPPS remain unclear. Numerous studies have indicated that HMGB1 can activate the NF-κB signaling cascade by interacting with receptors like advanced glycation end products (RAGE), toll-like receptor 2 (TLR2), and TLR4. This activation results in the upregulation and subsequent secretion of pro-inflammatory cytokines such as IL-1β, IL-2, and TNF-α, from monocytes, macrophages, neutrophils, and other immune cells. These inflammatory factors, in turn, can stimulate immune cells to secrete HMGB1, creating a positive feedback loop within a certain range.[17,18] This feedback loop may explain why CP/CPPS is difficult to treat, highlighting the importance of investigating the role of HMGB1 in the mechanisms of CP/CPPS.

Materials and Methods

Mice and EAP Induction

This experiment utilized male NOD mice, aged 6 to 8 weeks, obtained from the Jiangsu GemPharmatech Co., Ltd. (Jiangsu, China). Sprague-Dawley rats, weight 250 to 320g, obtained from Chongqing Enbi Biotechnology Co., Ltd (Chongqing, China). All experimental subjects were housed in a controlled, pathogen-free environment at the Animal Research Facility of Chongqing Medical University. The experimental procedures involving animals were scrutinized and subsequently endorsed by the Institutional Animal Care and Use Committee (IACUC) at the same institution (IACUC-SAHCQMU-2024-00058). The welfare of laboratory animals was ensured in accordance with the guidelines of the "Experimental Animal Welfare General Rules" (GB/T 42011–2022), and the "Guidelines for Ethical Review of Laboratory Animal Welfare" (GB/T 35892–2018). Additionally, the 3R principles (Replacement, Reduction, Refinement) were strictly followed to minimize the use of animals and reduce their suffering. The EAP mouse model was established following established methods.[19,20] Sprague-Dawley rats for the preparation of prostate protein antigens. After euthanasia, the rats' prostates were harvested, cleaned, and homogenized on ice using a grinder containing sterile PBS with an equal weight of 0.5% Triton X-100 (P0096, Beyotime Biotech, Jiangsu, China) and protease inhibitors. The supernatant was used to emulsify with complete Freund's adjuvant (CFA; Sigma--Aldrich, St. Louis, MO, USA) in a 1:1 ratio, forming a stable "water-in-oil" emulsion. This antigen

emulsion was used to immunize NOD mice at multiple subcutaneous sites (bilateral inguinal areas, shoulders, and tail base) with a total volume of 150 μL/mouse. Immunizations occurred on days 0 and 28, with the control group receiving CFA injections at the same sites.[21] Mouse-derived recombinant HMGB1 (rmHMGB1) protein (#50913, Sino Biological) was intraperitoneally injected daily at 500 ng/mouse for 14 consecutive days after the second immunization. The control group for HMGB1 experiments received an equal volume of 0.9% saline (vehicle for rmHMGB1). Glycyrrhizin (HY-N0184, MedChem Express), a small-molecule antagonist of HMGB1, was given intraperitoneally at 5 mg/kg daily for 14 days following the second immunization. The control group for glycyrrhizin experiments received the same solvent mixture (5% DMSO, 40% PEG300, 5% Tween 80, and 50% sterile water) without glycyrrhizin. The rmHMGB1 protein was dissolved in 0.9% saline, while glycyrrhizin powder was prepared in 100% DMSO as a stock solution and diluted to a working concentration using a mixture of 5% DMSO, 40% PEG300, 5% Tween 80, and 50% sterile water. On day 42 post-induction, mice were subjected to behavioral tests, then euthanized to collect blood and prostate tissues for subsequent analysis. Protein concentration was adjusted to 50 mg/mL and stored at −80°C.

Cell Culture

RAW264.7 cells were obtained from CAS Cell Bank (Shanghai, China). RAW264.7 cells were cultured in DMEM (high glucose) with 10% FBS, 1% penicillin-streptomycin, and maintained at 37°C, 95% humidity, and 5% CO_2. Unless specified otherwise, the LPS concentration used in experiments with RAW264.7 cells was 1 μg/mL. For in vitro experiments, rmHMGB1 pretreatment was performed 3 h before LPS stimulation. The interference sequences that specifically targeted HMGB1 (si-HMGB1:5′-GACTATTAGGATCAAGCAA-3′) and a negative control (si-NC) siRNA were procured from RiboBio Co., Ltd. (Guangzhou, China). According to the manufacturer's instructions, RAW264.7 cells were transfected with si-HMGB1 (60 nM) or si-NC (60 nM) using Lipofectamine 2000 (Invitrogen).

Behavioral Test

Before euthanizing the mice, pain sensitivity was evaluated using the Von Frey mechanical pain test kit. As detailed in previous studies,[19,22] the pressure was focused on the periprostatic region, with care taken to vary the pressure sites to prevent desensitization. Before testing, the mice were allowed to adjust to their new surroundings for 30 minutes. Tactile allodynia and hyperalgesia were quantified using five distinct filaments exerting forces of 0.04, 0.16, 0.4, 1.0, and 4.0 g on each mouse. Filaments were applied for 1–2 seconds each, with 5-second intervals, 20 times in total. The incidence of positive responses was calculated and statistically compared. Three behavioral manifestations were considered as indicative of a positive response to the stimulus; 1) sharp abdominal retraction; 2) immediate licking or scratching at the site of filament application; 3) a leaping response.

Hematoxylin and Eosin (H&E) Staining

Paraffin-embedded tissues were sectioned at 5 μm thickness. Sections underwent sequential treatment with xylene, followed by a graded ethanol series (100%, 95%, 90%, 80%, 70%) and distilled water (dH_2O) for 5 minutes each to facilitate dewaxing and rehydration. Subsequently, sections were stained with hematoxylin and eosin in sequence. Microscopic images were obtained using a light microscope. Histological scoring, conducted blindly, assessed the extent of prostatic inflammation. Inflammation was scored on a four-point scale (0 to 3), as previously described.[23] 0, no inflammation; 1/Mild Single inflammatory cells, most of which are separated by distinct interstitial spaces; 2/Moderate Fused sheets of inflammatory cells without tissue destruction or lymphoid nodule/follicle formation; 3/Severe Clusters of inflammatory cells with tissue destruction or lymphoid nodule/follicular formation.

Immunofluorescence

Paraffin-embedded prostate tissue sections were dewaxed, rehydrated, and subjected to antigen retrieval in EDTA buffer (pH 8.0) using a 90°C water bath for 30 minutes with natural cooling, and subsequent PBS washes. Endogenous peroxidase activity was quenched with 3% H_2O_2 and non-specific binding blocked with 5% BSA for 30 min. The sections were then incubated overnight at 4°C with primary antibodies anti-HMGB1 (1:5000, GB11103; Servicebio),

anti-CD11b (1:5000, GB15058; Servicebio), anti-E-cadherin (1:2000, GB11082; Servicebio), anti-iNOS (1:2500, GB11119; Servicebio) After three washes with PBS, the slides were incubated at room temperature for 50 minutes with an HRP-conjugated goat anti-rabbit IgG secondary antibody (1:500, GB23303; Servicebio). TSA signal amplification was performed by sequential incubation with iF488-Tyramide (1:500, G1231; Servicebio), CY3-Tyramide (1:500, G1223; Servicebio). Finally, the nuclei were counterstained with DAPI for 10 minutes, and the slides were visualized using an Olympus FV3000 microscope. For cellular immunofluorescence staining, cellular fixation was conducted in situ on the slides for 30 minutes with 4% paraformaldehyde. Subsequently, the slides were processed following the above procedures. The slides were incubated overnight at 4°C with the iNOS antibody (1:100; DF7113; Affinity). After three rinses with PBST, the slides were incubated with Cy3 goat anti-rabbit secondary antibody (1:500, A0516; Beyotime). Finally, the cells were visualized using an Olympus FV3000 microscope.

RNA Isolation and Reverse Transcription-Quantitative Polymerase Chain Reaction (RT-qPCR)

Total RNA extraction from RAW264.7 cells was performed using TRIzol reagent (GlpBio, GK20008) following the manufacturer's protocol. RNA purity and concentration were assessed with a NanoDrop 2000 spectrophotometer (NanoDrop Technologies). Reverse transcription was conducted using the PrimeScript™ RT reagent kit (Takara, Kusatsu, Japan). Quantitative PCR (qPCR) was set up in a final volume of 20 μL using SYBR Green Mix (Takara, Kusatsu, Japan) with primers synthesized by Sangon Biotech (Sangon, Shanghai, China). Amplification and detection were carried out on an ABI7500 platform (Thermo, MA, USA). Relative gene expression was quantified using the $2^{-\Delta\Delta CT}$ method, and GAPDH was used as an internal control to normalize the data. Each reaction was repeated four times. The following primer sequences were used for RT-qPCR: HMGB1 (forward) 5′-GGCGAGCATCCTGGCTTATC -3′. HMGB1 (reverse) 5′-GGCTGCTTGTCATCTGCTG-3′; GAPDH (forward) 5′-AGGTCGGTGTGAACGGATTTG-3′. GAPDH (reverse) 5′-TGTAGACCATGTAGTTGAGGTCA-3′.

Western Blot Assays

Western blot analysis involved extracting total cellular protein using Beyotime Biotech lysis buffer (Jiangsu, China), supplemented with a comprehensive inhibitor cocktail and PMSF. Denaturation was achieved by 30-minute incubation at 95°C, followed by separation on 12.5% SDS-PAGE and transfer to polyvinylidene fluoride (PVDF) membranes. After 1-hour blocking with 5% skim milk at room temperature, membranes were incubated with primary antibodies overnight at 4°C. The following primary antibodies were used: anti-HMGB1 antibody (1:500, AF7020; Affinity), anti-TRAF6 antibody (1:500, AF5376; Affinity), anti-IL-6 antibody (1:1000, DF6087; Affinity), anti-iNOS antibody (1:2000, 80,517-1-RR; Proteintech), anti-TNF-α antibody (1:500, AF7014; Affinity), NF-κB p65 (1:1000, #8242; CST), phospho-NF-κB p65 (1:1000, #3033; CST), GAPDH (1:5,000, 10,494-1-AP; Proteintech), and α-tubulin (1:5,000, AF7010; Affinity). After washing, the membranes were incubated with secondary antibodies for 2 hours. Visualization was achieved using BeyoECL Moon (P0018FS, Beyotime Biotech, Jiangsu, China). The band density was quantified using the Image J software (National Institutes of Health).

Enzyme-Linked Immunosorbent Assay (ELISA)

Serum concentrations of IL-6 and TNF-α in mice were measured utilizing ELISA kits specified for IL-6 (CSB-E04639m) and TNF-α (CSB-E04741m), both sourced from Cusabio. The assays were conducted in strict accordance with the protocols supplied by the manufacturer.

Protein Immunoprecipitation Assay

RAW264.7 cells were transfected with siRNA targeting HMGB1, followed by stimulation with LPS (1 μg/mL) and MG132 (0.35 μM) for 6 hours. Cells were lysed in immunoprecipitation lysis buffer with protease inhibitors and PMSF, incubated on ice for 30 minutes, and centrifuged at 12,000 × g for 15 minutes at 4°C. For immunoprecipitation, 1 mg of protein was incubated with TRAF6 antibody (4 μL, AF5376; Affinity) overnight at 4°C, and the remaining lysate was

used as the input control. Protein A/G magnetic beads (40 μL, #A1002; Abmart) were added and incubated overnight at 4°C, followed by four-time PBS washes. Immunoprecipitated proteins were eluted using SDS-PAGE loading buffer mixed with IP lysis buffer, heated at 95°C for 10 minutes, and analyzed by Western blot.

Statistical Analysis

Statistical analysis was performed using unpaired, two-tailed Student's *t*-test for comparison between two groups, and a one-way ANOVA with Bonferroni post hoc test was used for comparison among multiple groups. A two-way ANOVA analysis of variance was used to compare the two-factor experimental data. The Kruskal-Wallis nonparametric test was used to compare ranked data among multiple groups. GraphPad Prism version 6.0 software (GraphPad Software, San Diego, CA) was used for all the analyses. Results are expressed as mean ± standard deviation (SD). $P < 0.05$ was considered statistically significant. In the figures, "ns" indicates $P > 0.05$; *indicates $P < 0.05$; **indicates $P < 0.01$; ***indicates $P < 0.001$;****indicates $P < 0.0001$.

Results

HMGB1 Is Upregulated in the Prostate of EAP Mice

To investigate the expression changes and spatial localization of HMGB1 in prostate of EAP mice, co-immunofluorescence analysis was performed. The results showed significant co-localization of HMGB1 with macrophage marker CD11b (Figure 1A) and epithelial cell marker E-cadherin (Figure 1B) in the mouse prostate. The average fluorescence intensity of HMGB1 in macrophages and epithelial cells was compared in the prostate of EAP mice versus normal mice. We found a higher intensity of HMGB1 in both macrophages and epithelial cells in the prostate of EAP mice versus that of the normal mice (Figure 1C). The result was further corroborated by Western blot, and showed significantly elevated HMGB1 levels in prostate of EAP mice (Figure 1D and E). Since macrophages, particularly the M1 subtype, are key players in inflammatory responses, their role in HMGB1 expression was further examined in vitro. M1 macrophages were stimulated with LPS, and HMGB1 levels were measured over time. The results demonstrated a time-dependent increase in HMGB1 expression in M1 macrophages (Figure 1F and G). These results indicated that HMGB1 is highly expressed in both EAP mice and M1 macrophages, suggesting a potential role of HMGB1 in driving the inflammatory and pathological processes of CP/CPPS.

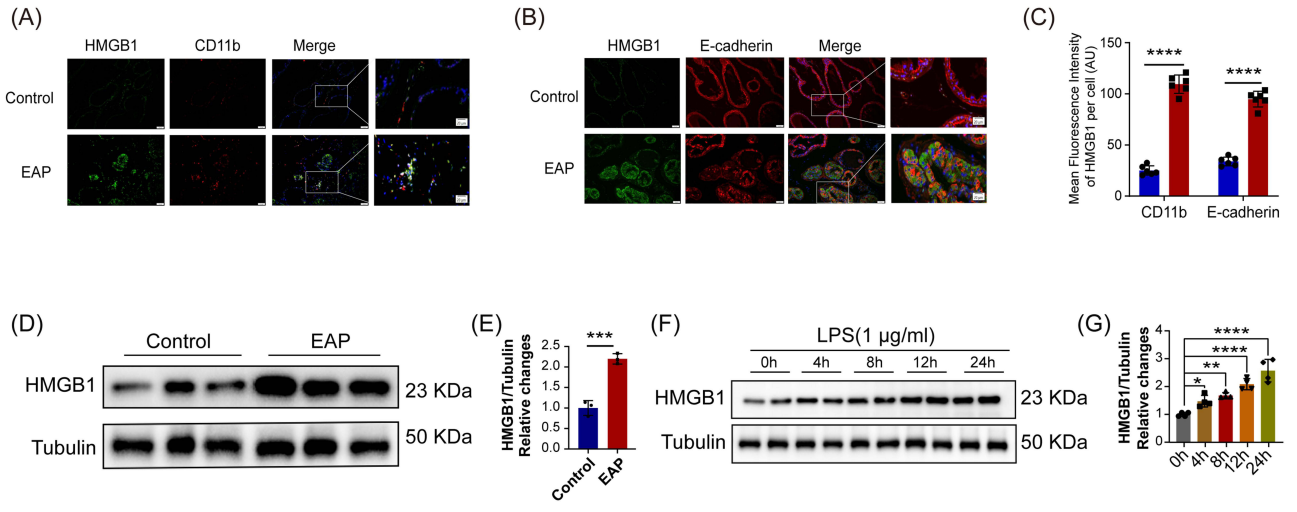

Figure 1 HMGB1 is increased in the prostate of EAP mice. Representative images of immunofluorescence staining for HMGB1 and markers of macrophage (**A**) and prostate epithelial cell (**B**). (**C**) Quantification of HMGB1 immunofluorescence intensity for macrophages and prostate epithelial cells in the prostate from the normal and EAP groups (n=6). (**D** and **E**) Western blot analysis of HMGB1 protein in the prostate tissues from the normal and EAP groups (n=3). (**F** and **G**) The HMGB1 protein levels at 0 h, 4 h, 8 h, 12 h and 24 h after LPS-stimulated RAW264.7 were detected by Western blot and quantified (n=4). Data are shown as mean ± SD, and analyzed by unpaired, two-tailed Student's *t*-test analysis (**C** and **E**) or one-way ANOVA analysis (**G**). *$P < 0.01$; **$P < 0.01$; ***$P < 0.001$; ****$P < 0.0001$.

https://doi.org/10.2147/JIR.S502616

HMGB1 Promotes the Progression of EAP by Enhancing M1 Polarization of Macrophages

To clarify whether HMGB1 promotes the progression of EAP by enhancing M1 polarization of macrophages, rmHMGB1 was administered. H&E staining revealed significantly higher inflammatory cell infiltration in the prostates of rmHMGB1-treated mice compared to the EAP group (Figure 2A), with elevated histopathological scores (Figure 2B). Behavioral assessments showed significantly increased pain responses to mechanical stimulation in rmHMGB1-treated mice, indicating heightened pain sensitivity (Figure 2C). To clarify the changes in the number of M1 macrophages in prostate tissue, we employed co-immunofluorescence analyses of iNOS and CD11b. The results demonstrated a notable increase in M1 macrophage numbers in the rmHGB1 group (Figure 2D and E). Previous studies have highlighted the critical roles of pro-inflammatory cytokines IL-6 and TNF-α in the pathogenesis of CP/CPPS.[24–26] Activated M1 macrophages are known to secrete these cytokines.[27] Consistent with this, we found significantly elevated levels of IL-6 (Figure 2F) and TNF-α (Figure 2G) in the rmHMGB1-treated group. These findings suggest that HMGB1 contributes to inflammatory progression and chronic pain in EAP mice by promoting M1 macrophage polarization.

Suppression of HMGB1 Ameliorates EAP by Inhibiting M1 Polarization of Macrophages

To investigate the therapeutic potential of HMGB1 inhibition in EAP mice, the HMGB1 antagonist glycyrrhizin was used. H&E staining demonstrated a significant reduction in the number of infiltrating inflammatory cells in the prostate of glycyrrhizin-treated mice (Figure 3A). Correspondingly, histopathological scores in the glycyrrhizin-treated group were significantly reduced (Figure 3B). Moreover, these mice exhibited a significantly lower frequency of pain responses to mechanical stimuli, suggesting a reduction in pain sensitivity (Figure 3C). Co-immunofluorescence staining for iNOS and CD11b revealed a notable decrease in M1-type macrophage numbers in the glycyrrhizin-treated group compared to the EAP group (Figure 3D and E). Furthermore, the levels of pro-inflammatory cytokines IL-6 (Figure 3F) and TNF-α

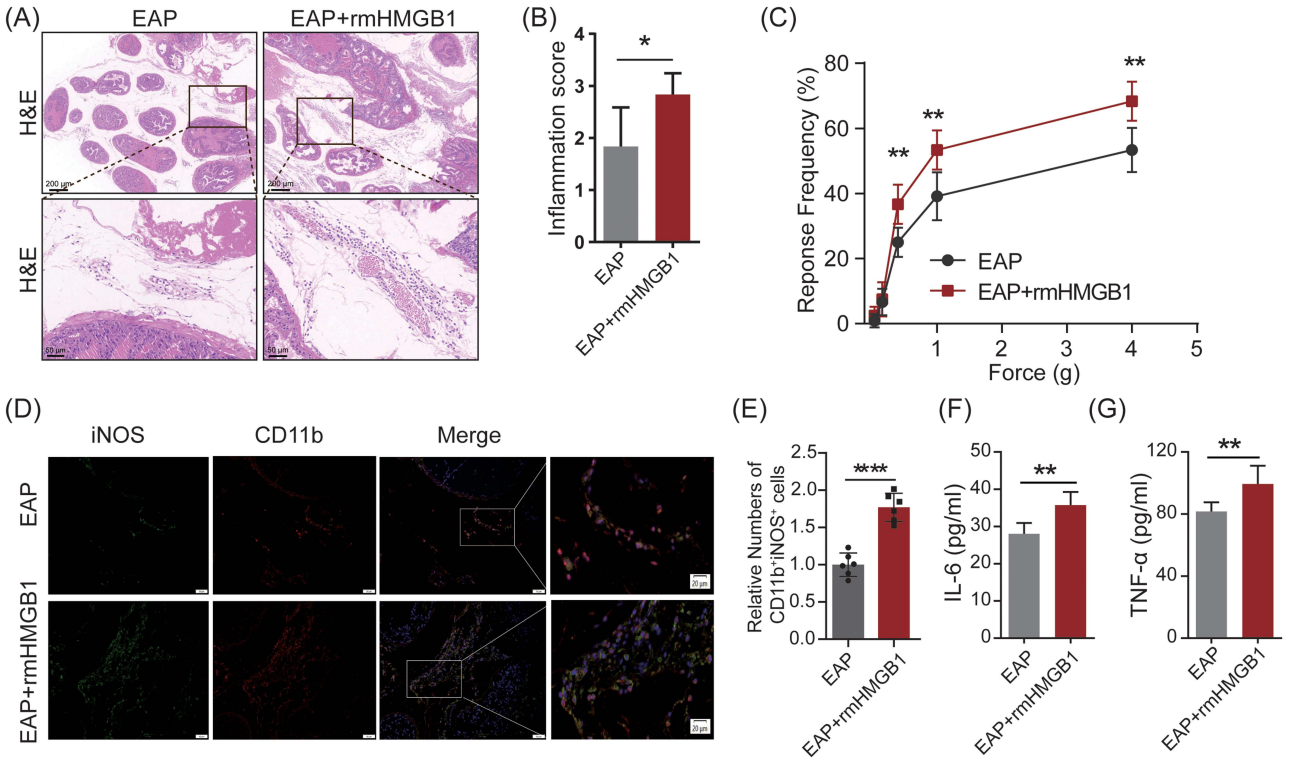

Figure 2 HMGB1 Promotes EAP severity. (**A**) Histological evaluation for the degree of inflammation for mice in the EAP and rmHMGB1 treatment groups. (**B**) The inflammation score for mice in the EAP and rmHMGB1 treatment groups (n=6). (**C**) Pain response test for mice in the EAP and rmHMGB1 treatment groups. (**D**) Representative images of immunofluorescence staining for iNOS and CD11b in the prostate of EAP and rmHMGB1 treatment mice. Cells were stained for iNOS (green) and CD11b (red). (**E**) Relative quantification of the numbers of $CD11b^{+}iNOS^{+}$ cells in prostate from EAP and rmHMGB1 treatment groups (n=6). (**F** and **G**) The expression levels of IL-6 and TNF-α in serum from EAP and rmHMGB1 treatment groups. Data are shown as mean ± SD, and analyzed by unpaired, two-tailed Student's *t*-test analysis (**B, E, F** and **G**) or two-way ANOVA analysis (**C**). **P* < 0.01; ***P* < 0.01; *****P* < 0.0001.

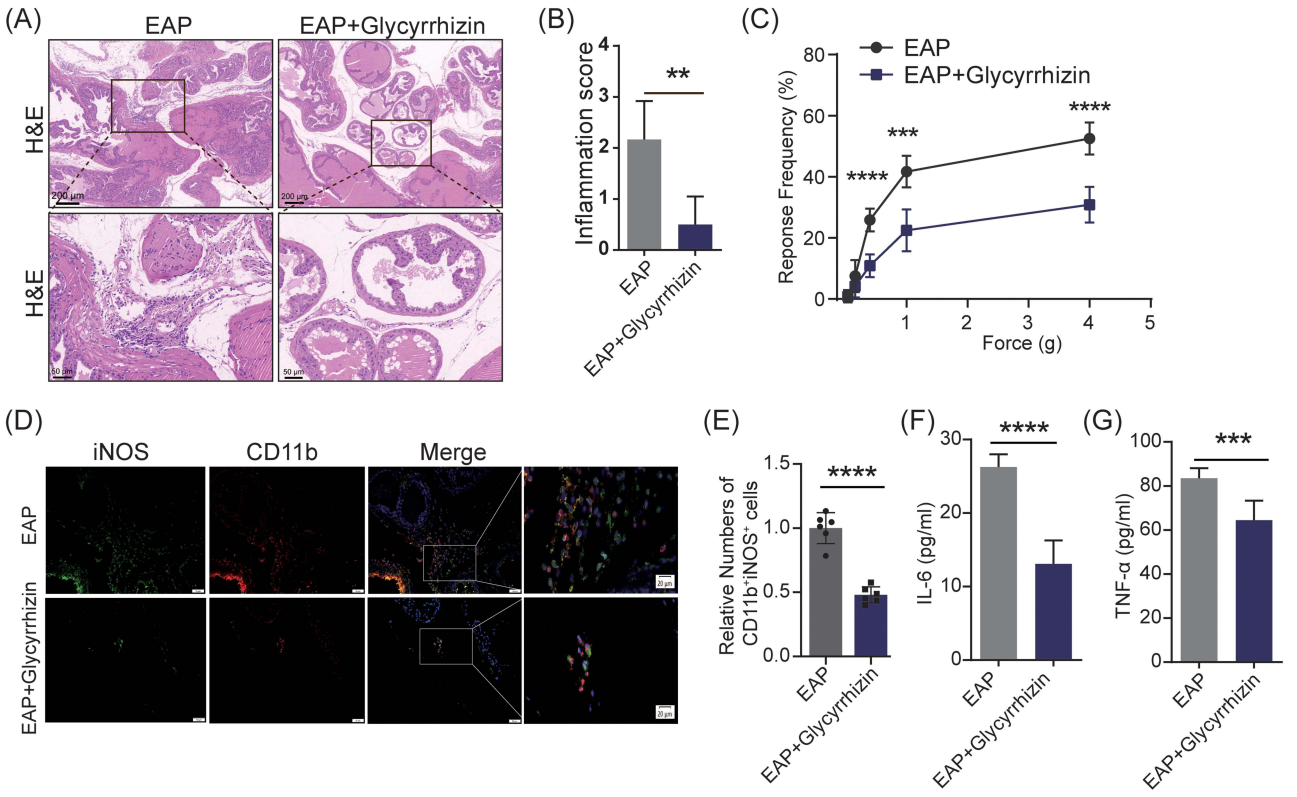

Figure 3 Suppression of HMGB1 with glycyrrhizin ameliorates EAP severity. (**A**) Histological evaluation for the degree of inflammation for mice in the EAP group and glycyrrhizin treatment group. (**B**) The inflammation score for mice in the EAP group and glycyrrhizin treatment group (n=6). (**C**) Pain response test for mice in the EAP group and glycyrrhizin treatment group (n=6). (**D**) Representative images of immunofluorescence staining for iNOS and CD11b in the prostate of EAP and glycyrrhizin treatment mice. Cells were stained for iNOS (green) and CD11b (red). (**E**) Relative quantification of the numbers of $CD11b^{+}iNOS^{+}$ cells in prostate from EAP and glycyrrhizin treatment group (n=6). (**F** and **G**) The expression levels of IL-6 and TNF-α in serum from EAP and glycyrrhizin treatment groups (n=6). Data are shown as mean ± SD, and analyzed by unpaired, two-tailed Student's *t*-test analysis (**B, E, F** and **G**) or two-way ANOVA analysis (**C**). $^{**}P < 0.01$; $^{***}P < 0.001$; $^{****}P < 0.0001$.

(Figure 3G) were significantly reduced in the glycyrrhizin-treated group. These findings suggest that glycyrrhizin mitigates EAP severity by reducing M1 macrophage polarization in vivo.

HMGB1 Promotes the Secretion of Inflammatory Mediators of Macrophages via TRAF6/NF-κB Activation

To explore the molecular mechanisms underlying HMGB1-mediated macrophage polarization, we conducted in vitro experiments using RAW264.7 cells pretreated with different concentrations of rmHMGB1 (250 ng/mL or 500 ng/mL) followed by LPS (1 μg/mL) stimulation. Western blot analysis revealed that iNOS expression was increased after rmHMGB1 treatment with LPS (Figure 4A and B). Similarly, the levels of pro-inflammatory cytokines IL-6 and TNF-α were also elevated in these groups (Figure 4A, C and D). Immunofluorescence further confirmed the significant upregulation of iNOS expression following rmHMGB1 treatment (Figure 4E). To investigate the potential mechanisms by which HMGB1 regulates M1 macrophage polarization, we utilized bioinformatics tools (http://string-db.org/) to analyze functional protein interactions, leading to the identification of several candidate proteins (Figure 4F). Among these candidates, TRAF6 stood out due to its involvement in a variety of inflammatory diseases.[28,29] Previous studies have established that TRAF6 plays a pivotal role in activating the NF-κB signaling pathway.[30] Activation of the TRAF6/NF-κB pathway is known to drive macrophage M1 polarization and enhance the release of inflammatory cytokines.[31] Based on these findings, we hypothesized that the HMGB1/TRAF6/NF-κB signaling pathway may promote macrophage M1 polarization and cytokine release. To validate this hypothesis, we detected TRAF6, p-NF-κB, and NF-κB protein levels in LPS-activated RAW264.7 cells pretreated with rmHMGB1 (Figure 4G). We found that rmHMGB1 significantly increased the expression levels of TRAF6 and p-NF-κB (Figure 4H and I). To further validate whether TRAF6 is essential for HMGB1-mediated activation of the NF-κB signaling

https://doi.org/10.2147/JIR.S502616

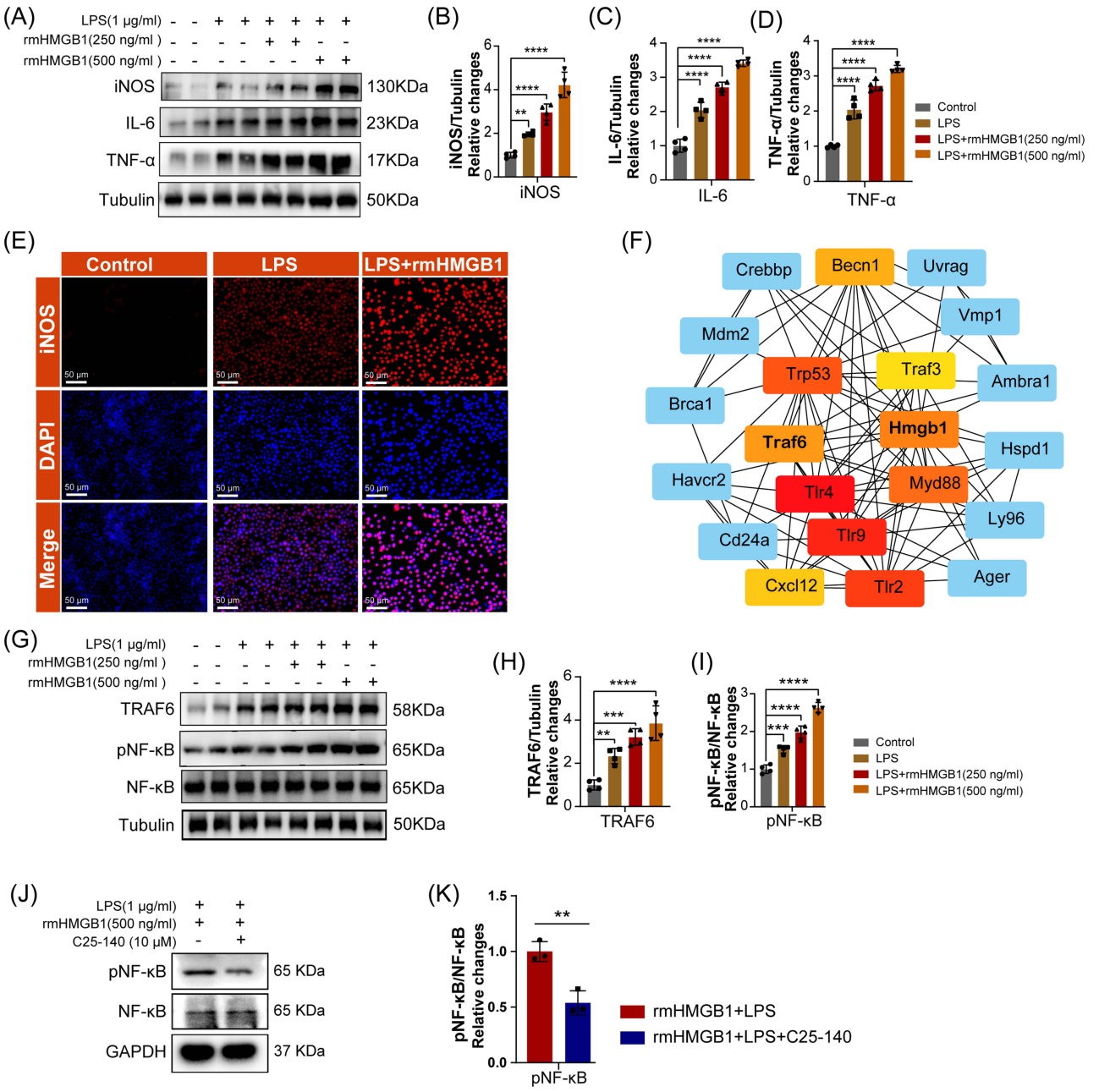

Figure 4 HMGB1 promotes M1 polarization of macrophages through TRAF6/NF-κB pathway. (**A**) Western blot was used to detect the protein levels of iNOS, IL-6 and TNF-α in RAW264.7 treated with rmHMGB1. Relative quantification of the protein levels of iNOS (**B**), IL-6 (**C**) and TNF-α (**D**) (n=4). (**E**) The iNOS was detected by immunofluorescence combined with DAPI staining for nuclei. (**F**) Protein-protein interaction diagram was performed by STRING website (http://string-db.org/). (**G**) Western blot was used to detect the protein levels of TRAF6, NF-κB, and pNF-κB in RAW264.7 treated with rmHMGB1. Relative quantification of the protein levels of TRAF6 (**H**), and pNF-κB (**I**) (n=4). (**J**) Western blot was used to detect the protein levels of pNF-κB and NF-κB in RAW264.7 pretreatment with the TRAF6-specific inhibitor C25-140 (10 μM) prior to rmHMGB1 and LPS treatment. (**K**) Relative quantification of the protein levels of pNF-κB (n=3). Data are shown as mean ± SD, and analyzed by unpaired, two-tailed Student's *t*-test analysis (**K**) or one-way ANOVA analysis (**B**, **C**, **D**, **H** and **I**). ***P* < 0.01; ****P* < 0.001; *****P* < 0.0001.

pathway, we performed functional rescue experiments using C25-140, a specific TRAF6 inhibitor. The experimental results demonstrated that C25-140 significantly suppressed the HMGB1-enhanced phosphorylation of NF-κB (Figure 4J and K). These findings suggest that HMGB1 promotes M1 macrophage polarization and the secretion of inflammatory mediators via the activation of the TRAF6/NF-κB pathway in vitro.

Silencing HMGB1 Prevents the Secretion of Inflammatory Mediators of Macrophages via TRAF6/NF-κB Pathway

To further confirm the hypothesis that HMGB1 promotes the secretion of inflammatory mediators by macrophages via the TRAF6/NF-κB pathway, HMGB1 expression was silenced in RAW264.7 cells using siRNA. RT-qPCR and Western blot analyses demonstrated successful knockdown of HMGB1 at both mRNA and protein levels (Figure 5A–C). Western blot analysis revealed reduced levels of HMGB1, iNOS, IL-6, and TNF-α in LPS-treated RAW264.7 cells following HMGB1 knockdown (Figure 5D–H), which was corroborated by immunofluorescence showing significantly decreased iNOS expression (Figure 5I). Further investigation of the TRAF6/NF-κB signaling pathway showed that HMGB1 silencing resulted in reduced levels of TRAF6 and p-NF-κB (Figure 5J–L). Notably, inhibition of TRAF6 with C25-140 further diminished NF-κB phosphorylation (Figure 5M and N). These findings further indicate that HMGB1 promotes M1 macrophage polarization and regulates the expression of pro-inflammatory mediators such as IL-6, TNF-α via the TRAF6/NF-κB pathway.

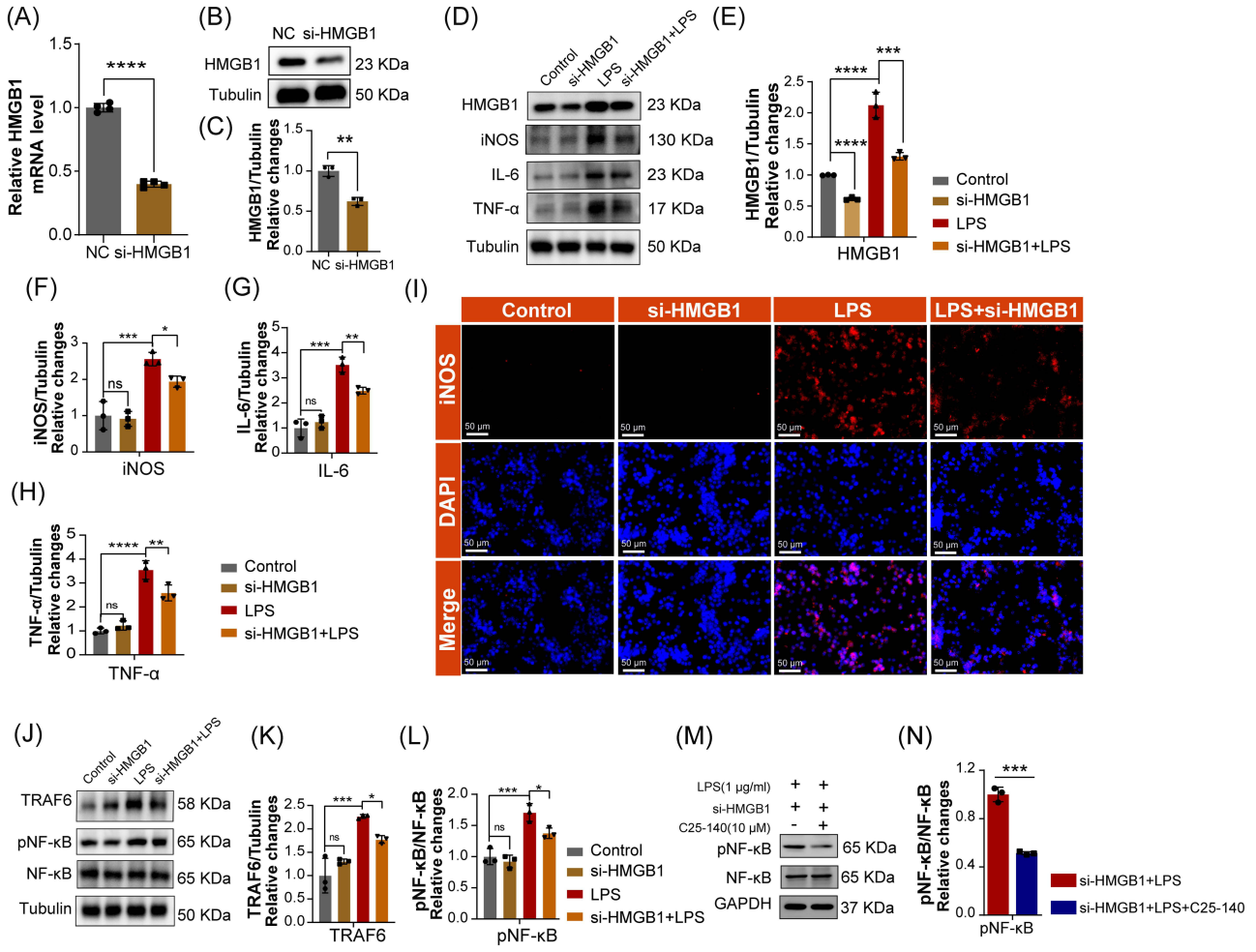

Figure 5 Silencing HMGB1 prevents the secretion of inflammatory mediators of macrophages via TRAF6/NF-κB pathway. (**A–C**) The silencing efficiency of HMGB1 in RAW264.7 was tested by RT-qPCR and Western blot. (**D**) Western blot was used to detect the protein levels of HMGB1, iNOS, IL-6 and TNF-α in si-HMGB1 group. Relative quantification of the protein levels of HMGB1 (**E**), iNOS (**F**), IL-6 (**G**) and TNF-α (**H**) (n=3). (**I**) The iNOS was detected by immunofluorescence combined with DAPI staining for nuclei. (**J**) Western blot was used to detect the protein levels of TRAF6, NF-κB, and pNF-κB in si-HMGB1 group. Relative quantification of the protein levels of TRAF6 (**K**), and pNF-κB (**L**) (n=3). (**M**) Western blot was used to detect the protein levels of pNF-κB and NF-κB in si-HMGB1 cells pretreatment with the TRAF6-specific inhibitor C25-140 (10 μM) prior to LPS stimulation. (**N**) Relative quantification of the protein levels of pNF-κB (n=3). Data are shown as mean ± SD, and analyzed by unpaired, two-tailed Student's *t*-test analysis (**C** and **N**) or one-way ANOVA analysis (**E**, **F**, **G**, **H**, **K** and **L**). **P* < 0.05; ***P* < 0.01; ****P* < 0.001; *****P* < 0.0001.

https://doi.org/10.2147/JIR.S502616

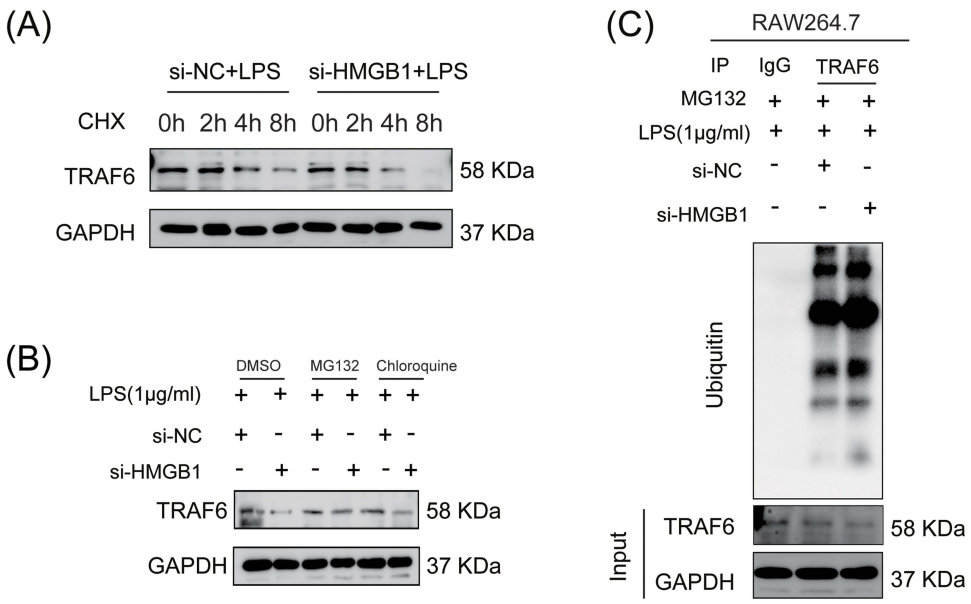

Figure 6 HMGB1 inhibited ubiquitination and degradation of TRAF6 protein. (**A**) TRAF6 protein was discerned by Western blot after treatment with CHX (20 μg/mL) at 0 h, 2 h, 4 h, 8 h in si-NC and si-HMGB1 cells in the presence of LPS. (**B**) TRAF6 protein was discerned by Western blot after treatment with MG132 (0.35 μM) and lysosomal inhibitor chloroquine (50 μM) in si-NC and si-HMGB1 cells in the presence of LPS. (**C**) Ubiquitination level of TRAF6 was detected by Western blot si-HMGB1 cells.

HMGB1 Inhibited Ubiquitination and Degradation of TRAF6

To investigate the potential regulatory mechanism of HMGB1 on TRAF6 protein, we performed a cycloheximide (CHX) chase assay to block new protein synthesis and assess the degradation rate and stability of TRAF6 protein. Time-course analysis revealed that TRAF6 degradation was significantly accelerated in HMGB1-silenced cells compared to controls (Figure 6A). These findings suggest that HMGB1 may stabilize TRAF6 by modulating its degradation process. To further elucidate the degradation pathway, we employed the proteasome inhibitor MG132 and the lysosomal inhibitor chloroquine. Notably, MG132 treatment effectively prevented TRAF6 degradation in HMGB1-silenced cells (Figure 6B), indicating that HMGB1 induced TRAF6 degradation primarily via the proteasomal pathway. Additionally, immunoprecipitation assays demonstrated a significant increase in TRAF6 ubiquitination upon HMGB1 silencing (Figure 6C). These findings collectively demonstrate that HMGB1 enhances TRAF6 protein stability by suppressing its ubiquitination and subsequent proteasomal degradation, thereby modulating TRAF6-dependent inflammatory signaling.

Discussion

In this study, we found that HMGB1 expression was markedly elevated in the prostate tissues of EAP mice. Treatment with rmHMGB1 exacerbated prostatic inflammation and pelvic pain, whereas administration of glycyrrhizin ameliorated prostatic inflammation and pelvic pain. Our results indicated that HMGB1 promotes macrophage polarization toward the M1 phenotype and enhances the secretion of pro-inflammatory mediators both in vivo and in vitro, thereby contributing to EAP pathogenesis. Mechanistically, HMGB1 activates the TRAF6/NF-κB signaling pathway, leading to a pro-inflammatory M1 phenotype in macrophages, which results in increased production of IL-6 and TNF-α. Notably, inhibition of TRAF6 with C25-140 significantly suppressed HMGB1-enhanced NF-κB phosphorylation, further supporting TRAF6's essential role in this pathway. Our findings suggest that HMGB1 can regulate TRAF6 activity via modulating its ubiquitination and degradation, thereby enhancing TRAF6-mediated NF-κB activation, driving M1 macrophage polarization, and ultimately exacerbating inflammatory responses.

CP/CPPS is a complex condition characterized by pelvic or perineal pain without evidence of urinary tract infection, lasting for at least 3 months.[32] Diagnosis of CP/CPPS primarily utilizes the NIH criteria, emphasizing symptom assessment, physical examinations, and exclusion of other urological conditions.[2] In this context, inflammatory markers such as C-reactive protein (CRP), IL-6, and TNF-α have emerged as potential biomarkers for diagnosing and gauging the severity of CP/CPPS.[33]

HMGB1 has been extensively studied as a contributor to the pathogenesis of various chronic inflammatory and autoimmune diseases. Elevated HMGB1 levels have been linked to the severity of inflammatory conditions such as rheumatoid arthritis,[34] systemic lupus erythematosus,[35] and sepsis.[36] In our study, we showed elevated HMGB1 expression in EAP mice and the pathogenic role of HMGB1 in EAP.

HMGB1 is predominantly localized in the nucleus of various cell types, such as macrophages and prostate epithelial cells, where it regulates critical cellular processes, including DNA organization, repair, and transcriptional regulation under physiological conditions. However, in response to inflammatory stimuli, immune cells undergo activation and actively release HMGB1 into the extracellular space, where it functions as a potent mediator of inflammation.[37] Once released into the extracellular space, HMGB1 serves as a damage-associated molecular pattern, binds to receptors such as RAGE, TLR4 and TLR2 on immune cells and perpetuates the inflammatory response.[18] This interaction enhances the inflammatory response, establishing HMGB1 as a key pro-inflammatory mediator. It plays a pivotal role in the development of various chronic inflammatory and autoimmune diseases including sepsis, rheumatoid arthritis, atherosclerosis, chronic kidney disease, and systemic lupus erythematosus. Moreover, HMGB1 has been implicated in mechanisms that promote cancer pathogenesis.[38] Our study suggests that HMGB1 can establish an inflammatory environment within the prostate by promoting M1 macrophage polarization and inducing the production of inflammatory cytokines. These results suggested that HMGB1-driven inflammation may be a pathogenic mechanism in CP/CPPS.

TRAF6, functioning as an intrinsic E3 ubiquitin ligase, directly catalyzes substrate ubiquitination through its RING domain. Mechanistically, TRAF6 is a key signaling mediator for the IL-1 receptor and TLR superfamily, coordinating cellular responses to cytokines and pathogen-associated molecular patterns (PAMPs).[30] Upon activation, these receptors recognize PAMPs and recruit the MYD88 adaptor protein, which subsequently leads to TRAF6 activation. Activated TRAF6 catalyzes K63-linked polyubiquitination of the TAK1 complex, forming a signaling scaffold that facilitates NF-κB activation via IκB kinase (IKK)-mediated phosphorylation.[39] Once activated, NF-κB translocates into the nucleus, driving the transcription of inflammatory mediators that promote M1 macrophage polarization.[31] Our data suggest that HMGB1 can enhance TRAF6 stability. HMGB1 can enhances TRAF6 protein expression by suppressing its ubiquitination and subsequent proteasomal degradation. In this study, we used C25-140, which directly binds to TRAF6, blocks its interaction with UBC13, and suppresses K63-linked ubiquitination. We found it significantly inhibited HMGB1-induced NF-κB activation. Based on our findings, we propose that HMGB1 primarily modulates TRAF6 function via the TLR4 pathway by regulating its K63-linked ubiquitination, thereby promoting downstream TAK1/NF-κB activation. Collectively, these findings indicate that HMGB1 may sustains inflammatory responses mainly by modulating TRAF6's ubiquitination and stabilizing TRAF6 protein.

Since HMGB1 plays a critical role in numerous inflammatory and autoimmune disorders, multiple inhibitory strategies have been proposed against HMGB1, such as HMGB1 monoclonal antibodies, small molecule inhibitors (eg Glycyrrhizin), and natural compounds (eg Epigallocatech-in-3-gallate).[38] Glycyrrhizin, a triterpene glycoconjugate derived from licorice roots, is known for its anti-inflammatory and antiviral effects. Studies have shown that glycyrrhizin binds to the HMG boxes of HMGB1 protein, effectively suppressing its chemotactic and cytokine activities.[40] Glycyrrhizin's therapeutic effects have been assessed in various inflammatory conditions, including inflammatory bowel diseases,[41] neuroinflammation and neurodegenerative disorders,[42] and radiation-induced lung injury.[43] Our study demonstrated the anti-inflammatory effect of glycyrrhizin in EAP mice. These findings underscore the broad therapeutic potential of glycyrrhizin and establish it as a promising candidate for clinical applications across a spectrum of inflammatory diseases.

Conclusions

This study establishes a critical role for HMGB1 in driving chronic prostatic inflammation via TRAF6/NF-κB axis-mediated M1 macrophage polarization, as mechanistically delineated in our proposed signaling paradigm (Figure 7). Targeting HMGB1 with glycyrrhizin is a promising approach to alleviate prostatic inflammation in CP/CPPS. This novel therapeutic strategy targeting HMGB1 may significantly improve treatment outcomes in CP/CPPS. However, further clinical trials are required to validate its clinical applicability.

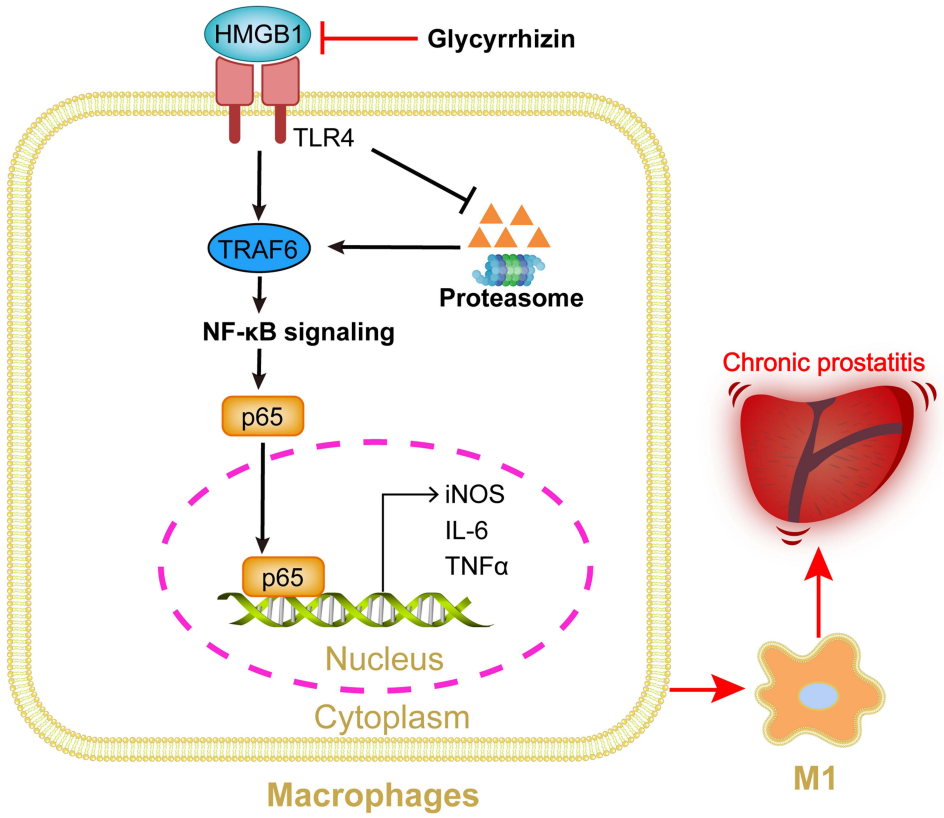

Figure 7 Schematic diagram of the pathogenicity of HMGB1 in mice with EAP. HMGB1 aggravates prostatic inflammation and pelvic pain in the EAP model by activating the TRAF6/NF-κB signaling to promote M1 polarization and the secretion of inflammatory mediators.

Data Sharing Statement

The data used to support the findings of this study are available from the corresponding author upon request.

Acknowledgments

This study was funded by Natural Science Foundation of Chongqing Science and Technology (CSTB2023NSCQ-BHX0040), Chongqing Postdoctoral Special Funding Projects (2023CQBSHTB3035), and Hubei Key Laboratory of Urological Diseases (MNXTJB202410) awarded to Xiaoliang-Hua.

Author Contributions

All authors made a significant contribution to the work reported, whether that is in the conception, study design, execution, acquisition of data, analysis and interpretation, or in all these areas; took part in drafting, revising or critically reviewing the article; gave final approval of the version to be published; have agreed on the journal to which the article has been submitted; and agree to be accountable for all aspects of the work.

Disclosure

The authors declare no conflicts of interest in this work.

References

1. Krieger JN, Lee SW, Jeon J, et al. Epidemiology of prostatitis. *Int J Antimicrob Agents*. 2008;31(Suppl 1):S85–90. doi:10.1016/j.ijantimicag.2007.08.028
2. Krieger JN, Nyberg L, Nickel JC. NIH consensus definition and classification of prostatitis. *JAMA*. 1999;282(3):236–237. doi:10.1001/jama.282.3.236

3. Baiyi L, Hongbin C, Wen H, et al. Protective effect of bamboo shoot oil on experimental nonbacterial prostatitis in rats. *Food Chem*. 2011;124(3):1017–1023. doi:10.1016/j.foodchem.2010.07.066
4. Clemens JQ, Mullins C, Ackerman AL, et al. Urologic chronic pelvic pain syndrome: insights from the MAPP research network. *Nat Rev Urol*. 2019;16(3):187–200. doi:10.1038/s41585-018-0135-5
5. Krsmanovic A, Tripp DA, Nickel JC, et al. Psychosocial mechanisms of the pain and quality of life relationship for chronic prostatitis/chronic pelvic pain syndrome (CP/CPPS). *Can Urol Assoc J*. 2014;8(11–12):403–408. doi:10.5489/cuaj.2179
6. De Marzo AM, Platz EA, Sutcliffe S, et al. Inflammation in prostate carcinogenesis. *Nat Rev Cancer*. 2007;7(4):256–269. doi:10.1038/nrc2090
7. Penna G, Mondaini N, Amuchastegui S, et al. Seminal plasma cytokines and chemokines in prostate inflammation: interleukin 8 as a predictive biomarker in chronic prostatitis/chronic pelvic pain syndrome and benign prostatic hyperplasia. *Eur Urol*. 2007;51(2):524–533. doi:10.1016/j.eururo.2006.07.016
8. Motrich RD, Maccioni M, Riera CM, Rivero VE. Autoimmune prostatitis: state of the art. *Scand J Immunol*. 2007;66(2–3):217–227. doi:10.1111/j.1365-3083.2007.01971.x
9. Steiner G, Gessl A, Kramer G, et al. Phenotype and function of peripheral and prostatic lymphocytes in patients with benign prostatic hyperplasia. *J Urol*. 1994;151(2):480–484. doi:10.1016/s0022-5347(17)34998-4
10. Kramer G, Steiner GE, Handisurya A, et al. Increased expression of lymphocyte-derived cytokines in benign hyperplastic prostate tissue, identification of the producing cell types, and effect of differentially expressed cytokines on stromal cell proliferation. *Prostate*. 2002;52(1):43–58. doi:10.1002/pros.10084
11. True LD, Berger RE, Rothman I, Ross SO, Krieger JN. Prostate histopathology and the chronic prostatitis/chronic pelvic pain syndrome: a prospective biopsy study. *J Urol*. 1999;162(6):2014–2018. doi:10.1016/S0022-5347(05)68090-1
12. John H, Barghorn A, Funke G, et al. Noninflammatory chronic pelvic pain syndrome: immunological study in blood, ejaculate and prostate tissue. *Eur Urol*. 2001;39(1):72–78. doi:10.1159/000052415
13. Ludwig M, Steltz C, Huwe P, et al. Immunocytological analysis of leukocyte subpopulations in urine specimens before and after prostatic massage. *Eur Urol*. 2001;39(3):277–282. doi:10.1159/000052453
14. Penna G, Amuchastegui S, Cossetti C, et al. Treatment of experimental autoimmune prostatitis in nonobese diabetic mice by the vitamin D receptor agonist elocalcitol. *J Immunol*. 2006;177(12):8504–8511. doi:10.4049/jimmunol.177.12.8504
15. Tang D, Kang R, Zeh HJ, Lotze MT. The multifunctional protein HMGB1: 50 years of discovery. *Nat Rev Immunol*. 2023;23(12):824–841. doi:10.1038/s41577-023-00894-6
16. Xue R, Xu J, Ma S, Jia Z, Yang J. High-mobility group box 1 is involved in the development of benign prostatic hyperplasia with chronic prostatic inflammation. *Scand J Urol*. 2015;49(6):479–485. doi:10.3109/21681805.2015.1059357
17. Ivanov S, Dragoi AM, Wang X, et al. A novel role for HMGB1 in TLR9-mediated inflammatory responses to CpG-DNA. *Blood*. 2007;110(6):1970–1981. doi:10.1182/blood-2006-09-044776
18. Dong Y, Ming B, Dong L. The role of HMGB1 in rheumatic diseases. *Front Immunol*. 2022;13(815257). doi:10.3389/fimmu.2022.815257
19. Breser ML, Motrich RD, Sanchez LR, Mackern-Oberti JP, Rivero VE. Expression of CXCR3 on specific T cells is essential for homing to the prostate gland in an experimental model of chronic prostatitis/chronic pelvic pain syndrome. *J Immunol*. 2013;190(7):3121–3133. doi:10.4049/jimmunol.1202482
20. Zhang LG, Chen J, Meng JL, et al. Effect of alcohol on chronic pelvic pain and prostatic inflammation in a mouse model of experimental autoimmune prostatitis. *Prostate*. 2019;79(12):1439–1449. doi:10.1002/pros.23866
21. Shen S, Wu Y, Chen J, et al. CircSERPINE2 protects against osteoarthritis by targeting miR-1271 and ETS-related gene. *Ann Rheum Dis*. 2019;78(6):826–836. doi:10.1136/annrheumdis-2018-214786
22. Rudick CN, Schaeffer AJ, Thumbikat P. Experimental autoimmune prostatitis induces chronic pelvic pain. *Am J Physiol Regul Integr Comp Physiol*. 2008;294(4):R1268–1275. doi:10.1152/ajpregu.00836.2007
23. Breser ML, Motrich RD, Sanchez LR, Rivero VE. Chronic pelvic pain development and prostate inflammation in strains of mice with different susceptibility to experimental autoimmune prostatitis. *Prostate*. 2017;77(1):94–104. doi:10.1002/pros.23252
24. Hu C, Yang H, Zhao Y, et al. The role of inflammatory cytokines and ERK1/2 signaling in chronic prostatitis/chronic pelvic pain syndrome with related mental health disorders. *Sci Rep*. 2016;6(1):28608. doi:10.1038/srep28608
25. Karlovsky ME, Pontari MA. Theories of prostatitis etiology. *Curr Urol Rep*. 2002;3(4):307–312. doi:10.1007/s11934-002-0055-y
26. Liu J, Yu J, Peng X. Poria cocos polysaccharides alleviates chronic nonbacterial prostatitis by preventing oxidative stress, regulating hormone production, modifying gut microbiota, and remodeling the DNA methylome. *J Agric Food Chem*. 2020;68(45):12661–12670. doi:10.1021/acs.jafc.0c05943
27. Manderson AP, Kay JG, Hammond LA, Brown DL, Stow JL. Subcompartments of the macrophage recycling endosome direct the differential secretion of IL-6 and TNFalpha. *J Cell Biol*. 2007;178(1):57–69. doi:10.1083/jcb.200612131
28. Matsumoto R, Dainichi T, Tsuchiya S, et al. Epithelial TRAF6 drives IL-17-mediated psoriatic inflammation. *JCI Insight*. 2018;3(15). doi:10.1172/jci.insight.121175
29. Vlantis K, Polykratis A, Welz PS, et al. TLR-independent anti-inflammatory function of intestinal epithelial TRAF6 signalling prevents DSS-induced colitis in mice. *Gut*. 2016;65(6):935–943. doi:10.1136/gutjnl-2014-308323
30. Dainichi T, Matsumoto R, Mostafa A, Kabashima K. Immune control by TRAF6-mediated pathways of epithelial cells in the EIME (Epithelial Immune Microenvironment). *Front Immunol*. 2019;10(1107). doi:10.3389/fimmu.2019.01107
31. Gohda J, Matsumura T, Inoue J. Cutting edge: TNFR-associated factor (TRAF) 6 is essential for MyD88-dependent pathway but not toll/IL-1 receptor domain-containing adaptor-inducing IFN-beta (TRIF)-dependent pathway in TLR signaling. *J Immunol*. 2004;173(5):2913–2917. doi:10.4049/jimmunol.173.5.2913
32. Khan FU, Ihsan AU, Khan HU, et al. Comprehensive overview of prostatitis. *Biomed Pharmacother*. 2017;94:1064–1076. doi:10.1016/j.biopha.2017.08.016
33. Shoskes DA, Albakri Q, Thomas KIM, Cook D. Cytokine polymorphisms in men with chronic prostatitis/chronic pelvic pain syndrome: association with diagnosis and treatment response. *J Urol*. 2002;331–335. doi:10.1097/00005392-200207000-00100
34. Taniguchi N, Kawahara K, Yone K, et al. High mobility group box chromosomal protein 1 plays a role in the pathogenesis of rheumatoid arthritis as a novel cytokine. *Arthritis Rheum*. 2003;48(4):971–981. doi:10.1002/art.10859

35. Abdulahad DA, Westra J, Bijzet J, et al. High mobility group box 1 (HMGB1) and anti-HMGB1 antibodies and their relation to disease characteristics in systemic lupus erythematosus. *Arthritis Res Ther*. 2011;13(3):R71. doi:10.1186/ar3332
36. Wang H, Bloom O, Zhang M, et al. HMG-1 as a late mediator of endotoxin lethality in mice. *Science*. 1999;285(5425):248–251. doi:10.1126/science.285.5425.248
37. Gardella S, Andrei C, Ferrera D, et al. The nuclear protein HMGB1 is secreted by monocytes via a non-classical, vesicle-mediated secretory pathway. *EMBO Rep*. 2002;3(10):995–1001. doi:10.1093/embo-reports/kvf198
38. Musumeci D, Roviello GN, Montesarchio D. An overview on HMGB1 inhibitors as potential therapeutic agents in HMGB1-related pathologies. *Pharmacol Ther*. 2014;141(3):347–357. doi:10.1016/j.pharmthera.2013.11.001
39. Deng L, Wang C, Spencer E, et al. Activation of the IkappaB kinase complex by TRAF6 requires a dimeric ubiquitin-conjugating enzyme complex and a unique polyubiquitin chain. *Cell*. 2000;103(2):351–361. doi:10.1016/s0092-8674(00)00126-4
40. Mollica L, De Marchis F, Spitaleri A, et al. Glycyrrhizin binds to high-mobility group box 1 protein and inhibits its cytokine activities. *Chem Biol*. 2007;14(4):431–441. doi:10.1016/j.chembiol.2007.03.007
41. Leite CDS, Bonafe GA, Carvalho Santos J, et al. The anti-inflammatory properties of licorice (Glycyrrhiza glabra)-derived compounds in intestinal disorders. *Int J Mol Sci*. 2022;23(8):4121. doi:10.3390/ijms23084121
42. Song JH, Lee JW, Shim B, et al. Glycyrrhizin alleviates neuroinflammation and memory deficit induced by systemic lipopolysaccharide treatment in mice. *Molecules*. 2013;18(12):15788–15803. doi:10.3390/molecules181215788
43. Chai Y, Wang Z, Li Y, et al. Glycyrrhizin alleviates radiation-induced lung injury by regulating the NLRP3 inflammasome through endoplasmic reticulum stress. *Toxicol Res*. 2024;13(1):tfae009. doi:10.1093/toxres/tfae009